

Compressible Turbulent Boundary-Layer Heat Transfer to Rough Surfaces in Pressure Gradient

KARL K. CHEN*

Avco Systems Division, Wilmington, Mass.

The velocity defect law and the law of wall for nonadiabatic compressible turbulent boundary layers on rough wall are presented in terms of the generalized velocities suggested by Van Driest. It is possible to correlate measured boundary-layer profiles, for a range of Mach number from 0 to 5 and wall temperature ratio T_w/T_{aw} from 1.0 to 0.5, on the universal curves. From these correlations, the skin friction law for rough surfaces under various Mach number, heat-transfer rate and pressure gradients is generated. The corresponding heat-transfer relation is derived from the established incompressible semiempirical correlations based on the model that roughness effects on the mixing process is restricted to a relatively small region near the wall. The resulting equations are combined with the momentum integral equation and an auxiliary equation to provide a calculation method for predicting the development of the compressible turbulent boundary layer over rough surfaces in pressure gradient. The analysis is compared with a series of heat-transfer measurements on roughened hemispheres at Mach number 5 and 6. The agreement in general is good.

Nomenclature

A	= constant in velocity defect law, c.f. Eq. (3)
A_g	= parameter in generalized velocity, c.f. Eq. (1)
B	= sublayer Stanton number, c.f. Eq. (11)
B_g	= parameter in generalized velocity, c.f. Eq. (1)
\bar{B}	= constant in law of wall, c.f. Eq. (6)
C	= roughness spacing effect, c.f. Eq. (7)
C_f	= skin friction coefficient
F	= entrainment parameter, c.f. Eq. (33)
G^*	= generalized defect shape parameter, c.f. Eq. (4)
H	= shape factor, c.f. Eq. (29)
H_1	= entrainment shape factor, c.f. Eq. (32)
\bar{H}	= transformed shape factor, c.f. Eq. (36)
h	= enthalpy
h_s	= stagnation enthalpy
h_t	= friction enthalpy, c.f. Ref. 22
j	= 0 or 1 for two dimensional or axisymmetric flow
k	= roughness height
\bar{K}	= molecular conductivity
M	= Mach number
P_r	= molecular Prandtl number, $P_r = C_p \mu / \bar{K}$
P_t	= turbulent Prandtl number
q	= heat flux
r	= radius from the axis of symmetry
r_c	= recover factor
Re_∞/ft	= Reynolds number per feet ahead of shock
T	= temperature
U_τ	= friction velocity
U^*	= generalized velocity, c.f. Eq. (1)
U, V	= velocity components along and normal to the surface
x, y	= Cartesian coordinates along and normal to the surface
γ	= perfect gas constant
Δ^*	= generalized turbulent boundary-layer thickness, c.f. Eq. (2)
ΔU_1	= shift of velocity profile in the law of wall (6), due to surface roughness
δ	= boundary-layer thickness
δ^*	= displacement thickness, c.f. Eqs. (30)

δ_k^*	= kinematic displacement thickness, $\int_0^\infty \left(1 - \frac{U}{U_e}\right) dy$
ϵ, ϵ_h	= eddy viscosity and conductivity
θ	= momentum thickness
κ	= universal constant in law of wall and defect law, 0.41, c.f. Eqs. (3) and (6)
λ	= roughness density
μ	= viscosity
ν	= kinematic viscosity
ρ	= density
τ	= shear stress

Subscripts

aw	= adiabatic wall
e	= outer edge of boundary layer
h	= outer edge of roughness sublayer
k	= kinematic
s	= stagnation
w	= wall
∞	= ahead of shock

Introduction

THE role played by rough surfaces in fluid mechanics has been of interest for a long time, because of its decisive effect on many important aerodynamic characteristics such as the laminar-turbulent transition, the surface drag and the aerodynamic heating. The effect of surface roughness on these characteristics is of great practical importance in the fields of aerospace, marine, and hydraulic engineering. Recent developments in re-entry technology have indicated two kinds of surface roughness according to the mechanism of formation. For materials containing 3-D woven fibers, the orthogonal fibers protrude into the flow when the surface ablates and develop surface roughness of the same order as the fiber dimension, typically ranging from 10 to 40 mils. Roughness elements of that size are usually larger than the corresponding laminar boundary layer thickness, and trip the boundary layer to turbulent flow even at the neighborhood of the stagnation point. The second kind of roughness is induced under supersonic turbulent boundary layers by the naturally formed cross-hatching phenomena which has been observed on a wide variety of heat shield materials including among others, Teflon, phenolics, plastics, camphor, and even woods.^{2,3} The roughness elements whose sizes sometimes may reach as high as 50 mils³ are located some distance away from the stagnation point and

Presented as Paper 71-166 at the AIAA 9th Aerospace Sciences Meeting, New York, January 25-27, 1971; submitted March 15, 1971; revision received December 10, 1971. The work was partially supported by the Air Force Space and Missiles Systems Organization under Air Force Contract F04701-69-C-0117. The author wishes to acknowledge A. Pallone and N. Thyson for suggesting this problem and B. L. Reeves for many fruitful discussions during the course of this work.

Index category: Boundary Layers and Convective Heat Transfer—Turbulent.

* Staff Scientist. Member AIAA.

are not directly responsible for the original tripping of the boundary layers to turbulent flows. However, both types of roughness increase by a significant amount the heat flux and shear stress, which in turn cause considerable increases of surface ablation rates. In the past, the method for predicting the development of turbulent boundary layers over rough surfaces were few, and most were restricted to the cases of zero pressure gradient and of incompressible flow. No methods have been published for the predictions of compressible turbulent heat transfer to rough surfaces under arbitrary pressure gradient. Since most regions of interest on the nose of re-entry vehicles have a pressure gradient and the development of roughness could start even at the stagnation point,³³ the objective of this paper is to develop a method to predict heat flux under such situations.

The earliest studies on roughness effects were conducted by Nikuradse⁴ in pipe flows, with the drag being estimated from the easily measurable head losses. Under the assumption that the roughness effect is universal and independent of outside-flow conditions, Prandtl and Schlichting⁵ have derived the skin-friction relation for sand roughened plates from the Nikuradse's pipe data. More recently, the works of Morris,⁶ Bettermann,⁷ Liu et al.,⁸ and Perry et al.¹⁰ have included the effect of the spacing between roughness elements on the resistance and on the flow fields close to the wall. Based on the experimentally determined skin friction law, Dvorak⁹ was able to predict the development of turbulent boundary layers over rough surfaces in arbitrary pressure gradient with the integral entrainment method originally proposed by Head.¹¹ As to the incompressible turbulent heat transfer to rough surfaces, Dipprey and Sabersky¹³ and Owen and Thomson¹⁴ have independently proposed two very similar models based on the idea that the mechanism of heat transfer over rough surfaces is dominated by the scouring action over surfaces by eddying fluid. In both methods, a sublayer Stanton number is introduced and related empirically to the roughness Reynolds number and Prandtl number. Recently, Nestler¹⁵ has employed the semiempirical correlation of Owen and Thomson to supersonic flows. However, measurements for compressible turbulent flow over rough surfaces were few and most were limited to adiabatic cases. The experimental study of roughness effects at supersonic flows by Goddard¹⁶ indicated that the skin friction drag is a function of only the roughness Reynolds number based on the fluid properties close to the wall, exactly as in the incompressible case. The effect of compressibility is indirectly exhibited in the reduction of density at the wall as Mach number increases.

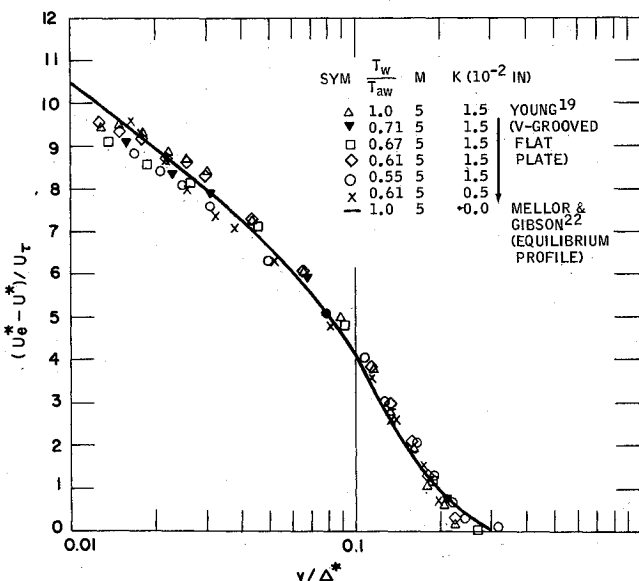


Fig. 1 Generalized velocity defect for nonadiabatic compressible turbulent boundary layers on rough surfaces.

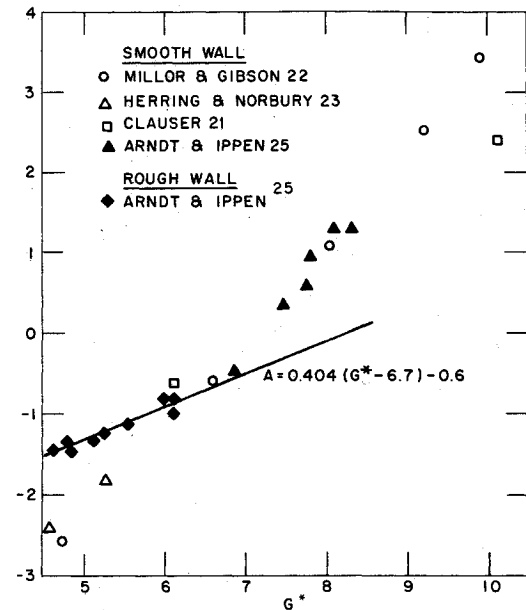


Fig. 2 Correlation of pressure gradient effect with shape factor.

The present approach attempts to extend the applicability of the relatively well established incompressible skin-friction law and heat-transfer relations to compressible flows. Both the velocity-defect law and the law of the wall of compressible turbulent boundary layers will be discussed. A calculation procedure is then proposed, which enables a prediction to be made for the development of the compressible turbulent boundary layer over rough surfaces with pressure gradient.

Generalized Velocity Defect Law

For incompressible turbulent boundary layers, the universal curves of velocity-defect law or the law of wall provide good representations of boundary-layer velocity profiles. For compressible flows, especially for cases with heat transfer, similar profile curves which adequately represent the boundary layer in the wall region or in the outer region are not yet well established. After examining a series of adiabatic compressible turbulent boundary layers with Mach number ranging from 1.5 to 5, Maise and McDonald¹⁷ found that the data in velocity defect form can be correlated on a single curve, which follows the incompressible velocity-defect law, provided that the measured velocity is replaced by Van Driest's generalized velocity U^* ,¹⁸ i.e.,

$$U^* = \frac{U_e}{A_g} \left[\sin^{-1} \frac{2A_g^2 (U/U_e) - B_g}{(B_g^2 + 4A_g^2)^{1/2}} + \sin^{-1} \frac{B_g}{(B_g^2 + 4A_g^2)^{1/2}} \right] \quad (1)$$

where

$$A_g^2 = [(\gamma - 1)/2] M_e^2 / (T_w/T_e)$$

$$B_g = \{1 + [(\gamma - 1)/2] M_e^2\} / (T_w/T_e) - 1$$

They also showed that the agreement of nonadiabatic velocity profile with the correlation curve is not so good as the adiabatic cases. A logical extension of this transformation would be to the rough wall turbulent boundary layer. Recent measurements of Young¹⁹ were made at Mach 5 on V-grooved flat plates with roughness height up to 0.015 inches under cooled wall conditions, covering a range of T_w/T_{aw} from 0.5 to 1. Figure 1 presents the data of Young¹⁹ in terms of the generalized velocity defect; i.e. $(U_e^* - U^*)/U_\tau$ vs y/Δ^* , where Δ^* is the length parameter proposed by Clauser for incompressible flow with the substitution of U^* for U , i.e.,

$$\Delta^* \equiv \int_0^\infty (U_e^* - U^*)/U_\tau dy \quad (2)$$

It is seen that the data for rough wall compressible flows

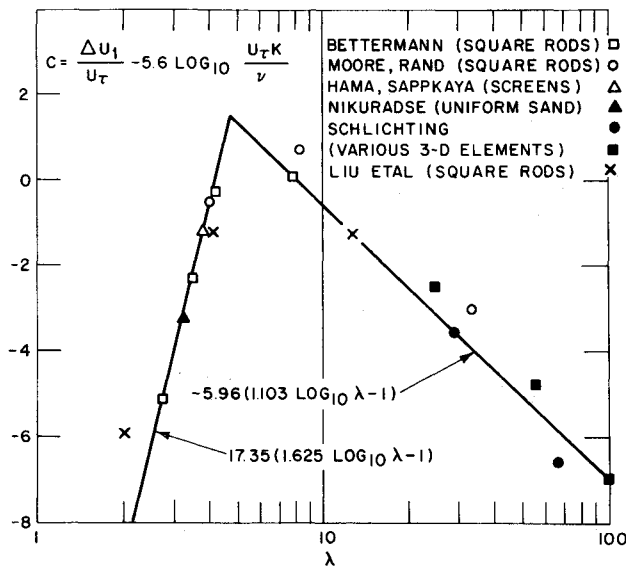


Fig. 3 The effect of roughness density on the law of wall intercept (from Ref. 9).

fall within a band following the universal curve of Clauser, which is obeyed by the incompressible turbulent flows of both smooth and rough walls.²⁰

Because of the limitation of the existing rough wall measurements, it does not seem possible to be able to analyze the relationship between Van Driest scaling and rough wall flow field in more detail. Therefore, in order to provide a method of calculation useful as an engineering analysis of this complex technical problem, the correlation in Fig. 1 will be used, i.e.,

$$(U_e^* - U^*)/U_\tau = -1/k \ln(y/\Delta^*) + \bar{A}(y/\Delta^*) \quad (3)$$

where k is a universal constant of 0.41 and \bar{A} approaches a constant A , as $y/\Delta^* \rightarrow 0$, indicating the relative location of the logarithmic portion of the velocity profile. According to Fig. 1, A appears to be independent of roughness size, heat transfer rate and Mach number. However, it can still be a function of the pressure gradient and the previous development, or the history of the boundary layer. The only correlation that appears possible at the moment is to express A as a function of some defect shape factor like G , which has been suggested by Clauser²¹ to characterize the various universal equilibrium profiles under different pressure gradients. With the use of the velocity U^* in the same way as for the generalized velocity-defect law of Eq. (3), the defect shape factor is defined as

$$G^* = \frac{\int_0^\infty (U_e^* - U^*)^2 / U_\tau^2 dy}{\int_0^\infty (U_e^* - U^*) / U_\tau dy} \quad (4)$$

It is further assumed that the dependence of Eq. (3) on G^* is identical to that of the incompressible velocity-defect law on G , which has been well established by Clauser²¹ and Mellor and Gibson²² in the studies of equilibrium flows. Figure 2 shows the correlation between A and G^* , including the numerical results of Mellor and Gibson,²² the experimental results of Clauser²¹ and of Herring and Norbury,²³ and the rough wall data of Arndt and Ippen.²⁴ It is indicated that the roughness elements have some consistent effects on the relation between A and G^* . Unfortunately the dependence of such effects on the roughness size is still not clear at the present stage. However, for fully rough region, the empirical formula suggested by Arndt and Ippen²⁴ (c.f. Fig. 2) that

$$A = 0.404(G^* - 6.7) - 0.6 \quad (5)$$

is used for rough estimations for the pressure gradient effect on the flow field over rough surfaces.

Law of Wall and of Skin Friction

Goddard¹⁶ has carried out an experimental program to study the effect of uniformly distributed sand-grain roughness on the skin-friction drag and on the boundary-layer flowfield for compressible flows with Mach numbers ranging from 0.7 to 5. It was indicated that the data for compressible flow fit the incompressible logarithmic law better when put in the form of Van Driest's generalized velocity than when presented in the form of actual velocity. The shift in the turbulent velocity profile due to roughness at supersonic speeds follows the same law as that for the incompressible case,¹⁶ i.e., a function of roughness Reynolds number kU_τ/v_w . Thus, the law of wall for compressible turbulent boundary layers over rough surfaces is

$$U^*/U_\tau = (1/k) \ln(yU_\tau/v_w) - (\Delta U_1/U_\tau) + \bar{B} \quad (6)$$

where $\Delta U_1/U_\tau$ represents the downward shift of the velocity profile in the vicinity of roughness elements, and \bar{B} is a constant indicating the location of the logarithmic portion of the smooth wall velocity profile. Clauser²¹ and others have shown that $\Delta U_1/U_\tau$ in the fully rough region, takes the form

$$\Delta U_1/U_\tau = 1/k \ln(U_\tau k/v_w) + C \quad (7)$$

where k is the physical roughness height and C is some function of the roughness geometry and density. Bettermann,⁷ using two-dimensional roughness elements of varying spacing, has correlated his own measurements as well as data from various sources, for the dependence of C on the roughness density, λ , which is defined as the ratio of total surface area to roughness area. For $1 < \lambda < 5$, the result is

$$C = 17.35(1.625 \log_{10} \lambda - 1) \quad (8)$$

as shown in Fig. 3. For roughness density greater than five, Dvorak⁹ was able to correlate the data from various sources in terms of Eq. (7) to have

$$C = -5.95(1.103 \log_{10} \lambda - 1) \quad (9)$$

which is also shown in Fig. 3. Numerically, Eqs. (8) and (9) are equal for a value of the roughness density $\lambda = 4.68$.

Experiments for compressible turbulent boundary layers on smooth surfaces have shown that the constant \bar{B} in Eq. (6), which indicates the location of the logarithmic portion of velocity profile plotted in the form of the law of wall, is a function of the heat-transfer rate or the wall temperature ratio.²⁵ In order to examine the effect of heat transfer rate on the displacement of the velocity profiles for rough wall, Fig. 4 presents the data of Goddard¹⁶ and Young¹⁹ with T_w/T_{aw} covering the range from 0.55 to 1. The scatter of the data, which is still

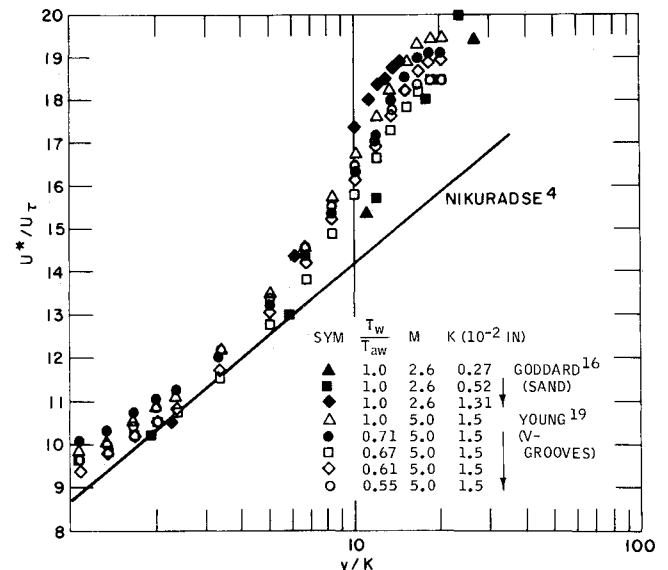


Fig. 4 Law of wall for nonadiabatic compressible turbulent boundary layers on rough surfaces.

tolerable in the standard of turbulent flow measurements, does not exhibit any apparent wall temperature ratio dependence. Hence a first-order approximation, the law of rough wall of Eq. (6) is considered to be independent of the heat transfer rate.

Substitution of Eqs. (3) into (6) leads to the generalized skin friction for rough surfaces,

$$U_e^*/U_\tau = 1/\kappa \ln(\Delta^*/k) + A(G^*) - C(\lambda) + \bar{B} \quad (10)$$

where, according to Clauser,²¹

$$\kappa = 0.41$$

$$\bar{B} = 4.9$$

and the dependence of A on G^* and of C on λ can be calculated from Eqs. (5) and (8) or (9), respectively.

Heat Transfer over Rough Surfaces

It is well known that the increase in the rate of heat transfer caused by rough surfaces exposed to a turbulent stream of fluid is less than the corresponding increase in skin friction. This can be explained qualitatively by the fact that the tangential forces are transmitted to the wall by pressure forces acting on the roughness elements while heat is not transferred by this process. This does not mean that the heat-transfer rate is independent of surface roughness, since eddies are developed around the crests of protuberances and draw fluid down into the valley like regions between adjacent roughness elements. The eddying fluid then scours over the solid surface before returning to mix with the main flow near the height of the roughness crests. As the scouring and mixing processes are the basic heat transfer mechanism,^{13,14} the small region near the wall may be regarded as a roughness dominated sublayer which has a characteristic velocity scale U_τ and a single length scale k . The experiments and analyses by Prandtl, Schlichting⁵ and Hama²⁰ for incompressible flow and by Goddard¹⁶ for compressible flow indicate that the roughness effect is independent of external flow conditions but is a function of the local flow conditions around the roughness elements. It is plausible to assume that the incompressible heat-transfer analyses by Dipprey and Sabersky¹³ and by Owen and Thomson¹⁴ in the roughness sublayer can be applied as well to the cases of compressible flows, provided the fluid properties are replaced by those at the wall conditions. Thus the rate of heat transfer across unit area of the layer is

$$q = \rho_w U_\tau (h_h - h_w) B \quad (11)$$

where h_h and h_w are the enthalpies at the outer edge of the sublayer and at the solid surface respectively, ρ_w is the density of the fluid at the wall and B is the sublayer Stanton number which is a function of the roughness Reynolds number and of the Prandtl number. By correlation of subsonic heat-transfer data, Owen and Thomson¹⁴ obtained the following expression for B ,

$$B = \frac{1}{\alpha} \left(\frac{\rho_w U_\tau k}{\nu_w} \right)^{-0.45} Pr^{-0.8} \quad (12)$$

where α varies between 0.45 and 0.7 with an average value of 0.52 and Pr is the molecular Prandtl number.

Before further discussions about the Reynolds analogy in the velocity and temperature defects, let us briefly review the mean boundary-layer equations for compressible turbulent flow,^{5,12} i.e.

$$\partial(\rho U r^j)/\partial x + \partial(\rho v r^j)/\partial y = 0 \quad (13)$$

$$\rho U (\partial U / \partial x) + \rho v (\partial U / \partial y) = -dp/dx + \partial \tau / \partial y \quad (14)$$

$$\rho U (\partial h_s / \partial x) + \rho v (\partial h_s / \partial y) = \partial(q + U\tau) / \partial y \quad (15)$$

where

$$\tau = \mu(\partial U / \partial y) - \rho \overline{U'v'} \quad (16)$$

$$q = \bar{K}(\partial h / \partial y) - \rho \overline{v'h'} \quad (17)$$

and

$$j = 0, \text{ for two dimensional flow} \\ 1, \text{ for axisymmetric flow}$$

The fluctuating terms in Eqs. (16) and (17) are usually much greater than the molecular viscosity and conductivity terms. Following Boussinesq,²⁶ the fluctuating terms are represented by forms which are analogous to the corresponding viscous and heat conduction terms. The shear stress and heat flux can then be approximated by

$$\tau \approx \varepsilon(\partial U / \partial y) \quad (18)$$

$$q \approx \varepsilon_h(\partial h / \partial y) \quad (19)$$

where ε and ε_h are called the eddy viscosity and eddy conductivity respectively.

Under the assumption of unity turbulent Prandtl number, Eq. (18) and (19) yield,

$$q + U\tau = \varepsilon(\partial h_s / \partial y) \quad (20)$$

For turbulent boundary layers in the fully rough region, all protrusions reach outside the laminar sublayer and the largest part of the resistance to flow is due to the form drag of the roughness. Since the form drag can increase indefinitely as the size of roughness element increase, the gradient of shear stress across the boundary layer can be much greater than the corresponding smooth wall value (c.f. Ref. 8). Thus the pressure gradient term in Eq. (14) is expected to be less significant for the rough wall than that for smooth wall. Substituting Eqs. (18) and (20) into Eqs. (14) and (15), respectively, the two equations are seen to be identical in form, if the pressure gradient term can be neglected. Thus h_s is expected to vary linearly with respect to U for constant wall temperature and the Reynolds analogy in terms of velocity and temperature defects¹⁴ is,

$$(h_{s,e} - h_s)/h_\tau = (U_e - U)/U_\tau \quad (21)$$

where

$$h_\tau \equiv q_w / \rho_w U_\tau \quad (22)$$

For incompressible heat transfer, the measurements of temperature profiles in a rough tube by Gowen and Smith²⁷ indicate that both $\rho U_\tau (h - h_w)/q_w$ and U/U_τ vary linearly with respect to $\log y/R$, and the slope of the temperature profile for air varies from 2.2 for a smooth wall to 2.7 for a rough wall while the slope of velocity profile remains constant at 2.5. Thus the approximate relation of Eq. (21) agrees with those measurements within 5%. Near the wall Eq. (21) becomes

$$(h_{s,e} - h_{s,h})/h_\tau = (U_e - U_h)/U_\tau \quad (23)$$

which, keeping in mind that $h_s \approx h$ in the wall region, can be combined with Eq. (11) to yield,

$$(h_{s,e} - h_w)/h_\tau = (U_e - U_h)/U_\tau + B^{-1} \quad (24)$$

where U_h is the streamwise mean velocity near the outer edge of the roughness sublayer. The difficulty in assigning a value to U_h has been discussed in detail by Owen and Thomson,¹⁴ who concluded that U_h/U_e is indistinguishable from zero and practically can be neglected. It follows from the substitution of Eqs. (22) into (24) that

$$q_w = \rho_w U_\tau^2 U_e^{-1} (h_{s,e} - h_w) / (1 + B^{-1} U_\tau U_e^{-1}) \quad (25)$$

Calculation Method

The momentum-integral equation for compressible flow is obtained by integrating Eqs. (13) and (14), that

$$\frac{d\theta}{dx} + (2 + H - M_e^2) \frac{\theta}{U_e} \frac{dU_e}{dx} + j \frac{\theta}{r} \frac{dr}{dx} = \frac{C_f}{2} \quad (26)$$

where

$$C_f \equiv 2\tau_w / \rho_e U_e^2 = (\rho_w / \rho_e) (U_\tau / U_e)^2 \quad (27)$$

$$\theta \equiv \int_0^\infty (\rho U / \rho_e U_e) (1 - U/U_e) dy \quad (28)$$

$$H \equiv \delta^*/\theta \quad (29)$$

and

$$\delta^* \equiv \int_0^\infty \left(1 - \frac{\rho U}{\rho_e U_e} \right) dy \quad (30)$$

The development of the compressible turbulent boundary layer on a rough surface with pressure gradient may be calculated using the momentum-integral equation in conjunction with the skin friction law in Eq. (10) and some auxiliary equation for the determination of the shape factor H . The auxiliary equation can be deduced empirically or semiempirically by using the energy-integral equation, the moment of momentum equation or the entrainment theory.²⁸ As pointed out by Dvorak,¹⁰ the auxiliary equations based on the shear integral or dissipation integral depend very much on conditions in the wall region, and the existing correlations must be reevaluated when the surface conditions are changed. Among the existing auxiliary equations, Head's entrainment equation seems most likely to be independent of conditions in the wall region. Thus, we select the entrainment method to avoid the complexity near the wall.

The main idea of Head's entrainment theory is to relate the shape parameter of the velocity profile to the rate at which fluid is entrained in the boundary layer.⁷ Integrating Eq. (13) across the boundary layer gives,

$$\frac{1}{\rho_e U_e r^j} \frac{d}{dx} \int_0^\delta \rho U r^j dy = \frac{1}{\rho_e U_e} \left(\rho_e U_e \frac{d\delta}{dx} - \rho_e v_e \right) \quad (31)$$

The expression within the brackets on the right hand side gives the mass rate (per unit area) at which fluid enters a control volume bounded at its upper surface by the edge of the boundary layer. For incompressible flow, Cumpsty and Head³¹ have denoted the right hand side of Eq. (31) by a dimensionless entrainment function F , which is simply a function of the shape parameter

$$H_1 \equiv (\delta - \delta^*)/\theta \quad (32)$$

Head⁷ has empirically established the quantitative relation between F and H_1 to which Standen³⁰ fitted the following equation,

$$F = 0.0306[(H_1)_i - 3]^{-0.653} \quad (33)$$

where the subscript i denotes incompressible flow. Green²⁹ extended Head's entrainment equation to compressible flow and reestablished the relation between entrainment and the shape parameter H_1 . He defined a corresponding kinematic shape parameter,

$$H_{1k} \equiv \int_0^\delta \left(\frac{U}{U_e} \right) dy / \int_0^\delta \left(\frac{U}{U_e} \right) \left(1 - \frac{U}{U_e} \right) dy \quad (34)$$

and argued that the entrainment parameter F and the shape parameter H_{1k} satisfy the empirical relation obtained by Head for incompressible flow. Thus $(H_1)_i$ in Eq. (33) shall be replaced by H_{1k} for compressible flow. Since Dvorak⁹ has shown that the surface roughness practically has no effect on the relation between F and $(H_1)_i$, Eqs. (31) and (33) can be used to describe the variation of shape factors for compressible turbulent flows over rough surfaces. Substitution of Eqs. (26) and (32) into Eq. (31) yields,

$$\frac{dH_1}{dx} = \frac{F}{\theta} + \frac{C_f H_1}{2\theta} + (H + 1) \frac{H_1}{U_e} \frac{dU_e}{dx} \quad (35)$$

which can be integrated simultaneously with Eqs. (26) and (10), if the auxiliary relations between shape factors such as H , H_1 , H_{1k} , and G^* are given. There are detailed discussions in both analytical and experimental approaches for the auxiliary relations among the shape factors such as H , H_1 , H_{1k} , and

$$\bar{H} \equiv \int_0^\delta (\rho/\rho_e) (1 - U/U_e) dy / \theta \quad (36)$$

in Ref. 29. The analyses of Green are based on the assumptions of a quadratic temperature distribution through the boundary layer, i.e.,

$$T/T_e = a_0 + a_1(U/U_e) + a_2(U/U_e)^2 \quad (37)$$

with

$$a_0 = T_w/T_e, \quad a_1 = (T_{aw} - T_w)/T_e, \quad a_2 = (T_e - T_{aw})/T_e$$

and of a power law velocity distribution,¹

$$U/U_e = (\bar{y}/\bar{\delta})^{1/n} \quad (39)$$

where

$$\bar{y} \equiv \int_0^y \frac{\rho}{\rho_e} dy \quad \text{and} \quad \bar{\delta} \equiv \int_0^\delta \frac{\rho}{\rho_e} dy$$

Following the same approach of Green, the following relations have been derived†:

$$H_{1k} = H_1 [a_0 + a_1(H_1 - 1)/H_1 + a_2(H_1 - 1)/(H_1 + 1)] / [a_0 + a_1(H_1 - 1)/(H_1 + 1) + a_2 H_1(H_1 - 1)/\{(H_1 + 1)(H_1 + 2)\}] \quad (40)$$

and

$$H = \bar{H}(T_w/T_e) + (T_{aw}/T_e) - 1 \quad (41)$$

The relation linking \bar{H} and H_1 is adopted from the empirical correlation of Green,

$$\bar{H} = 1 + [0.9/(H_1 - 3.3)]^{0.75} \quad (42)$$

The generalized length parameter in the skin friction law of Eq. (10) can be related to the transformed displacement thickness

$$\bar{\delta}^* \equiv \int_0^\infty \frac{\rho}{\rho_e} \left(1 - \frac{U}{U_e} \right) dy = \bar{H}\theta \quad (43)$$

By the combination of Eqs. (1, 2, 36, 37, 39, and 43), i.e.,

$$\frac{\Delta^*}{\bar{\delta}^*} = \frac{1}{A_g} \left(\frac{U_e}{U_\tau} \right) \left(\frac{\bar{H} + 1}{\bar{H} - 1} \right) \int_0^1 [\sin^{-1}(A_1 - B_1) - \sin^{-1}(A_1 \eta - B_1)] (a_0 + a_1 \eta + a_2 \eta^2) \eta^{(3-\bar{H})/(\bar{H}-1)} d\eta \quad (44)$$

where

$$A_1 = 2A_g^2/(B_g^2 + 4A_g^2)^{1/2}$$

and

$$B_1 = B_g/(B_g^2 + 4A_g^2)^{1/2}$$

The relation between G^* and \bar{H} is obtained by the combination of Eqs. (1, 4, 36, 37, and 39)

$$G^* = \left(\frac{U_e}{U_\tau} \right) \int_0^1 [\sin^{-1}(A_1 - B_1) - \sin^{-1}(A_1 \eta - B_1)]^2 \times (a_0 + a_1 \eta + a_2 \eta^2) \eta^{(3-\bar{H})/(\bar{H}-1)} d\eta / A_g \int_0^1 [\sin^{-1}(A_1 - B_1) - \sin^{-1}(A_1 \eta - B_1)] \times (a_0 + a_1 \eta + a_2 \eta^2) \eta^{(3-\bar{H})/(\bar{H}-1)} d\eta \quad (45)$$

Thus Eqs. (10, 26, and 35) with the auxiliary relations of Eqs. (40, 41, 42, 43 and 44) compose a determinate system of equations.

Calculation Procedure

Equations (26) and (35) are integrated simultaneously with the skin friction coefficient determined at each step in the calculation of Eq. (10). At the end of each step new values of H_1 and θ are obtained and local values of M_e , T_w , $(1/U_e)dU_e/dx$ and $(1/r)dr/dx$ are known. Then \bar{H} is evaluated from Eq. (36), H from (41), H_{1k} from (40), and finally F from (33). In order to calculate the skin-friction coefficient, G^* is evaluated from Eq. (45), Δ^* from Eq. (44), A from Eq. (5), C from Eqs. (8) and (9), U_e/U_e^* from Eq. (10), U_e^*/U_e from Eq. (1) and C_f from Eq. (27). The heat transfer rate to the rough wall can then be evaluated from Eq. (25) with B from Eq. (12). The forward integration of Eqs. (26) and (35) may now be taken a step further.

To start the calculation, initial values of θ and H are required. The behavior of numerical results indicates that, after a few steps of integration, they are rather insensitive to the

† At this point, we can actually follow the Van Driest transformation instead of introducing the velocity power law and Dorodnitsyn transformation. However, the procedures of the former approach is much more complicated than the latter. In view of the limitation of our present knowledge in the rough wall compressible flows, the author chose to follow a rather simple approach.

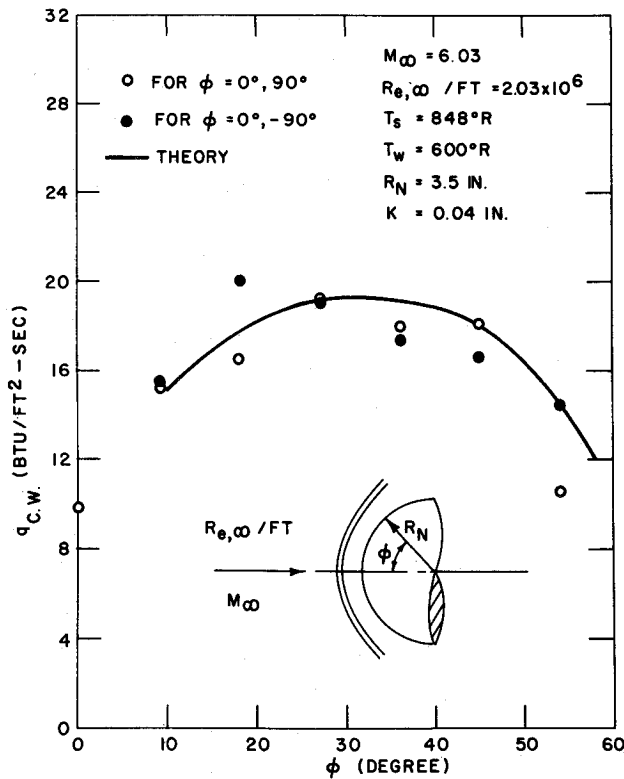


Fig. 5 Heat transfer to a very rough hemisphere.

starting values to be used.[‡] If the roughness height k is less than the corresponding laminar boundary-layer thickness, δ_{lam} , one may use the laminar θ and H to start with. However, if k is much greater than δ_{lam} , the initial value of θ should be of the same order of magnitude of k to avoid a breakdown of the numerical scheme. It should be noted that there are singular terms in the momentum integral Eq. (26) and the entrainment Eq. (35) at the stagnation point, where both the velocity U_e and axis radius r approach zero. More work is needed in modifying Eqs. (26) and (40) to allow starting from a stagnation point possible, since there is some evidence that the turbulent boundary layer could even start at a stagnation point if the surface is rough enough.³³

Comparison with Experiments

The effect of large scale roughness on heat transfer was investigated experimentally on rough hemisphere by Avco in a series of wind tunnel tests run at NOL ($M_\infty = 5$) and at AEDC ($M_\infty = 6$).³³ The hemispherical model had a radius of 3.5 in. Distributed roughness on the hemisphere was obtained by milling 0.04-in.-deep by 0.04-in.-wide grooves into the model surface in a regular pattern. The grooves extended from the stagnation point to a position of $\phi = 60^\circ$, where ϕ is the internal angle of the hemisphere measured from stagnation point. The roughness elements can be approximately considered as $0.04 \times 0.04 \times 0.04$ in. cubic blocks with the spacing between neighboring elements also equal to 0.04 in. Thus, the corresponding roughness density λ turns out to be a value of 4. The heat transfer data are presented in terms of cold-wall heat flux, i.e.,

$$q_{cw} \equiv q_w / (1 - h_w / h_{s,e}) \quad (46)$$

For calculation purpose, the inviscid flow properties at the outer edge of boundary layer are based on the modified Newton theory which gives reasonable accuracy for sphere at high Mach number³⁴ in the region between the stagnation point and

[‡] Similar behavior has been reported for integral methods for smooth wall (c.f., Ref. 32).

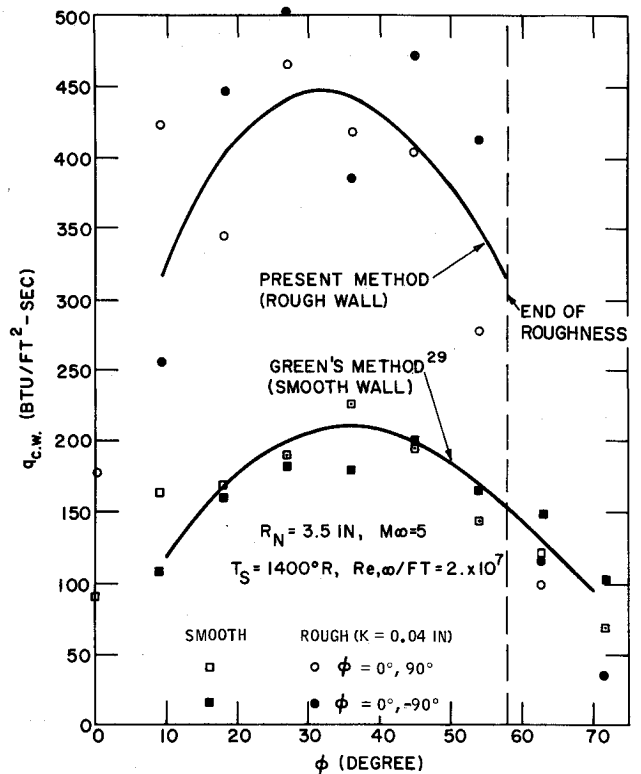


Fig. 6 Heat transfer to the hemisphere of very rough and smooth walls in a typical tunnel environment.

$\phi = 60^\circ$, where the roughness elements terminate.[§] Comparisons with the typical experimental results for the large scale roughness are shown in Figs. 5 and 6. The data appear to be rather scattered, but it is encouraging that the agreement between data and calculation is good. For comparison purpose, Fig. 6 presents also the corresponding smooth wall heat transfer data and calculations based on Green's method. Though the surface roughness appears to have remarkable effects on the magnitude of the heat-transfer rate, the heating distributions along both smooth and rough walls are seen to be rather similar to each

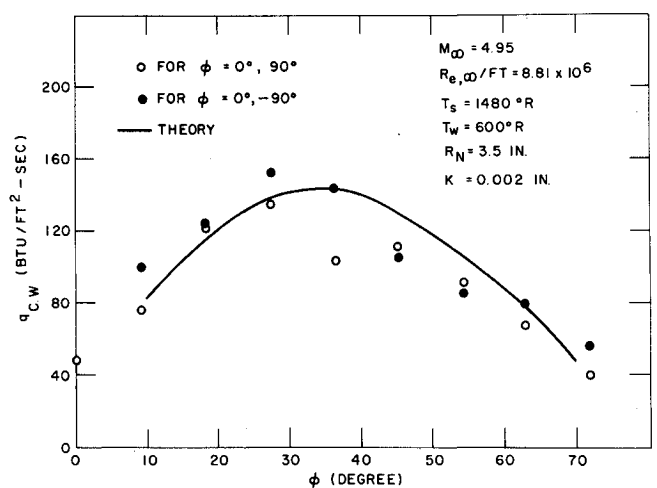


Fig. 7 Heat transfer to the hemisphere with intermediate roughness.

[§] Because of the increase of surface drag due to roughness, the values of the pressure gradient parameters $\beta_r \equiv \delta^*(dp/dx)\tau_w$ ^{21,35} of those calculations were found to be of the order of 10^{-2} , almost an order of magnitude smaller than the corresponding smooth wall values. According to the incompressible flow analysis of Ref. 35, these small pressure gradient parameters of that order would have negligible effects on the turbulent enthalpy profiles.

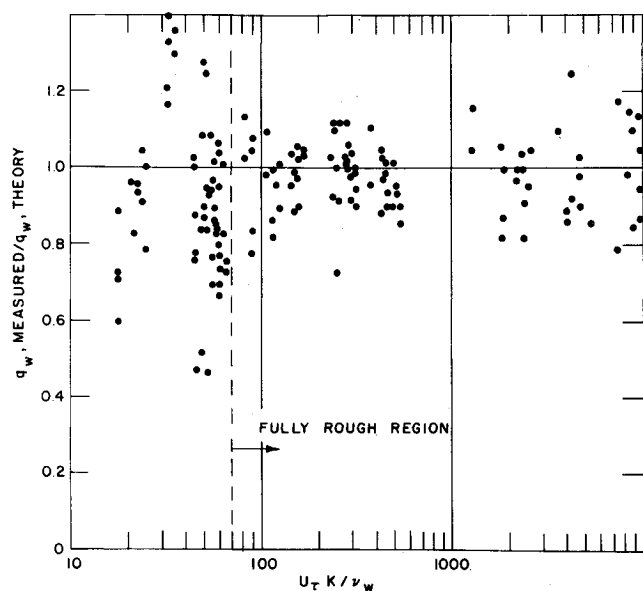


Fig. 8 Summary of the comparison between theory and experiments.

other; e.g., both having the maximum at about 35° of the internal angle ϕ . Thus, the rough wall dimensionless turbulent heating variables such as Stanton or Nusselt numbers are expected to have distributions similar to those of smooth wall except the magnitude, since the external edge conditions of boundary layers of both cases are equal to each other to the first order approximation.

Measurements were also made on hemispheres with intermediate random roughness surface finishes which were similar to 120 grit open-coat sandpaper with peak to valley roughness element heights about 0.002 in. The roughness density λ on such irregularly roughened surfaces is rather difficult to define. At the moment, we would assume it to be the same roughness density of the dense sand grain roughness used by Nikuradse, which Dvorak¹⁰ have specified equal to 3.17. Typical example of experimental results and theoretical calculations for intermediate roughness of 0.002 in. is presented in Fig. 7, and the agreement is again satisfactory. Figure 8 is a summary of the comparison between theory and experiment, where values of $\dot{q}_{\text{measured}}/\dot{q}_{\text{theory}}$ are plotted against the roughness Reynolds number, $U_\tau K/\nu_w$, for all rough wall measurements in Ref. 33. It clearly indicates that the scattering of points in the fully rough region is within $\pm 20\%$.

References

- Spence, D. A., "Velocity and Enthalpy Distributions in the Compressible Turbulent Boundary Layer on Flat Plate," *Journal of Fluid Mechanics*, Vol. 8, 1960, pp. 368-387.
- Langaneli, A. L. and Nestler, D. E., "Surface Ablation Patterns: A Phenomenology Study," *AIAA Journal*, Vol. 7, No. 7, July, 1969, pp. 1319-1325.
- Gold, H., Probstein, R. F., and Scullen, R. S., "Inelastic Deformation and Crosshatching," AIAA Paper 70-768, Los Angeles, Calif., 1970.
- Nikuradse, J., "Stromungsgesetze in rauhen Rohren," *VDI-Forschungsheft* 361, 1933; also TM 1292, 1950, NACA.
- Schlichting, H., *Boundary Layer Theory*, McGraw-Hill, New York, 1968.
- Morris, H. M., Jr., "Flow in Rough Conduits," *Transactions of the ASCE*, Vol. 120, 1955, pp. 373-397.
- Bettermann, D., "Contribution à l'Etude de la Convection Forcée Turbulente le Long de Plaques Rugueuses," *International Journal of Heat and Mass Transfer*, Vol. 9, 1966, pp. 153-164.
- Liu, C. K., "An Experimental Study of Turbulent Boundary Layer on Rough Walls," Ph.D. thesis, Aug. 1966, University Microfilms 67-4395, Stanford Univ., Palo Alto, Calif.
- Dvorak, F. A., "Calculation of Turbulent Boundary Layers on Rough Surfaces in Pressure Gradient," *AIAA Journal*, Vol. 7, No. 9, Sept. 1969, pp. 1752-1759.
- Perry, A. E., Schofield, W. H., and Joubert, P. N., "Rough Wall Turbulent Boundary Layers," *Journal of Fluid Mechanics*, Vol. 37, 1969, pp. 383-413.
- Head, M. R., "Entrainment in the Turbulent Boundary Layer," R and M 3152, 1958, Aeronautical Research Council, London, England.
- Reeves, B. L. and Baum, H., "Three-Dimensional Turbulent Boundary Layer Studies," AVSD-0210-70-RR, Vol. 1, Sept., 1970, Avco Systems Div., Wilmington, Mass.
- Dipprey, D. F. and Sabersky, R. H., "Heat and Momentum Transfer in Smooth and Rough Tubes at Various Prandtl Numbers," *International Journal of Heat and Mass Transfer*, Vol. 6, 1963, pp. 329-353.
- Owen, P. R. and Thomson, W. R., "Heat Transfer across Rough Surfaces," *Journal of Fluid Mechanics*, Vol. 15, 1963, pp. 321-334.
- Nestler, D. E., "Compressible Turbulent Boundary Layer Heat Transfer to Rough Surfaces," AIAA Paper 70-742, Los Angeles, Calif., 1970.
- Goddard, F. E., Jr., "Effect of Uniformly Distributed Roughness on Turbulent Skin-Friction Drag at Supersonic Speeds," *Journal of the Aerospace Sciences*, Vol. 20, No. 1, 1959, pp. 1-16.
- Maise, G. and McDonald, H., "Mixing Length and Kinematic Eddy Viscosity in a Compressible Boundary Layer," *AIAA Journal*, Vol. 6, No. 1, Jan. 1968, pp. 73-80.
- Van Driest, E. R., "Turbulent Boundary Layer in Compressible Fluids," *Journal of the Aeronautical Sciences*, Vol. 18, 1951, pp. 145-160.
- Young, F. L., "Experimental Investigation of the Effects of Surface Roughness on Compressible Turbulent Boundary Layer Skin Friction and Heat Transfer," DRL 532, AD621085, May 1965, Univ. of Texas, Austin, Texas.
- Hama, F. R., "Boundary Layer Characteristics for Smooth and Rough Surfaces," *Transactions 62, Naval Architects Marine Engineers*, 1954, pp. 91-108.
- Clauser, F. H., "Turbulent Boundaries in Adverse Pressure Gradient," *Journal of the Aeronautical Sciences*, Feb. 21, 1954, pp. 91-108.
- Mellor, G. L. and Gibson, D. M., "Equilibrium Turbulent Boundary Layers," *Journal of Fluid Mechanics*, Vol. 24, 1966, pp. 225-253.
- Herring, H. J. and Norbury, J. F., "Some Experiments on Equilibrium Turbulent Boundary Layers in Favorable Pressure Gradients," *Journal of Fluid Mechanics*, Vol. 27, No. 3, 1967, pp. 541-549.
- Danberg, J. E., "Characteristics of the Turbulent Boundary Layer with Heat and Mass Transfer at $M = 6.7$," TR 64-99, Oct. 1964, U. S. Naval Ordnance Lab., White Oak, Md.
- Arndt, R. E. and Ippen, A. T., "Cavitation Near Surfaces of Distributed Roughness," Rept. 104, 1967, Hydrodynamics Lab., MIT, Cambridge, Mass.
- Boussinesq, J., "Théorie de l'écoulement tourbillant," *Mémoires Présentés par Divers Savants à l'Académie des Sciences*, Vol. 23, 1877.
- Gowen, R. A. and Smith, J. W., "Turbulent Heat Transfer from Smooth and Rough Surfaces," *International Journal of Heat Mass Transfer*, Vol. 11, 1968, pp. 1657-1673.
- Rotta, J. C., "Recent Developments in Calculation Methods for Turbulent Boundary Layers with Pressure Gradients and Heat Transfer," *Journal of Applied Mechanics*, Vol. 33, No. 2, June 1966, p. 429.
- Green, J. E., "The Prediction of Turbulent Boundary Layer Development in Compressible Flow," *Journal of Fluid Mechanics*, Vol. 31, Pt. 4, 1968, pp. 753-778.
- Standen, N. M., "A Concept of Mass Entrainment Applied to Compressible Turbulent Boundary Layers in Adverse Pressure Gradients," *Proceedings of the 4th Congress of ICAS*, 1965, p. 1101.
- Cumpsty, N. A. and Head, M. R., "The Calculation of Three-Dimensional Turbulent Boundary Layers, Part I: Flow over the Rear of an Infinite Swept Wing," *Aeronautical Quarterly*, Vol. X, VII, 1967, p. 55.
- Sasman, P. K. and Cresci, R. J., "Compressible Turbulent Boundary Layer with Pressure Gradient and Heat Transfer," *AIAA Journal*, Vol. 4, No. 1, Jan. 1966, pp. 19-25.
- Otis, J. H., Jr., Rushton, G., Thyson, N., Howey, D., Chen, K. K., and DiCristina, V., "Nosetip Ablation Phenomena," AVSD-0210-70-RR, Vol. II, Avco Systems Div., Wilmington, Mass., Nov., 1970.
- Hayes, W. D. and Probstein, R. F., *Hypersonic Flow Theory*, Academic Press, New York, 1959.
- Alber, I. E. and Coats, D. E., "Equilibrium Enthalpy Profiles for the Incompressible Turbulent Boundary Layer with Heat Transfer," *AIAA Journal*, Vol. 9, No. 5, May 1971, pp. 791-796.